Ab initio calculation of the pleochroism of fayalite

O.V. Krasovska,[1,2] B. Winkler,[1] E.E. Krasovskii,[2] A.N. Yaresko,[2] V.N. Antonov,[2] and N. Langer[3]

[1]Mineralogisch-Petrographisches Institut der Christian-Albrechts Universität, Olshausenstrasse 40, D-24098 Kiel, Germany
[2]Institute of Metal Physics, National Academy of Sciences of Ukraine, Vernadskogo 36, 252680, Kiev-142, Ukraine
[3]Mineralogisches Institut, Technical University of Berlin, Ernst Reuter Platz 1, D-10587 Berlin, Germany

ABSTRACT

Optical properties of fayalite, Fe_2SiO_4, have been obtained from ab initio calculations on the basis of the self-consistent energy band structure. The semi-relativistic, extended linear-augmented plane wave method (ELAPW) was used. Comparison of the calculated polarized optical spectra with experimental absorbance spectra shows satisfactory agreement. This observation allows a semiquantitative interpretation of the origins of the observed d-d transitions. Energy level diagrams for Fe^{2+} ions in the M1 and M2 sites have been constructed using the Xα-scattered waves cluster method. These calculations quantitatively justify the use of the relationship $\Delta E \propto 1/R^5$, which is often used for the derivation of crystal-field stabilization energies at high pressures.

INTRODUCTION

The study of olivines is motivated by the fact that they are, with garnets and pyroxenes, the most important minerals in the Earth's upper mantle. Crystal chemical and structural properties of olivines have been reviewed by Brown (1982). The olivine structure can incorporate a large variety of 3d-transition metal ions. The influence of 3d-transition metal elements on the thermodynamic properties of minerals, through crystal field stabilization energies, is well known and recently was summarized by Burns (1993). The most common transition metal bearing olivine end-member is fayalite, Fe_2SiO_4. Fe-containing olivines have been the subject of several spectroscopic investigations (see review in Burns 1993); in particular, polarized (Burns 1970; Runciman et al. 1973) and unpolarized (Smith and Langer 1982) optical spectra of fayalite in visible and near-infrared region were measured. Because of their complex crystal structure, minerals pose a particular challenge for calculation of physical properties by ab initio methods. To our knowledge there have been no parameter-free quantum mechanical calculations of optical properties for minerals and no energy band structure calculations for fayalite.

The orthorhombic olivine structure belongs to the space group *Pbnm* and contains four Fe_2SiO_4 molecules per primitive cell. Atomic positional coordinates are listed in Table 1. Olivine contains discrete SiO_4 tetrahedra; all O atoms are bonded to just one Si atom. Each Fe atom is surrounded by a distorted octahedron of O atoms. The slightly smaller octahedron around the Fe1 site is centrosymmetric and its point symmetry is 1 (C_i) The slightly larger octahedron around the Fe2 site is acentric: Three Fe-O distances are significantly longer then the other three, and the octahedron is trigonally distorted. The point

symmetry of the Fe2 position is m (C_s). The experimental values of lattice parameters given by Schwab and Kustner (1977) are $a = 4.8211$, $b = 10.4779$, and $c = 6.0889$ Å. The crystal and optical axes relate by $\alpha \parallel b$, $\beta \parallel c$, $\gamma \parallel a$.

The polarized absorbance spectra of fayalite were measured by Burns (1970) in the region 0.5–3 eV. Fayalite is pleochroic: the mineral is pale yellow when the incoming light is parallel to a and b, and orange yellow when it is parallel to c. A distinctive feature of the γ spectrum is a very strong peak at 1.115 eV. The α and β spectra look similar, both having two broad peaks at ~1.00 and ~1.37 eV.

Burns (1970) treated the Fe1 and Fe2 sites in fayalite as having pseudo-tetragonal and pseudo-trigonal symmetry, respectively. On the basis of this assumption he proposed the energy level diagram for Fe^{2+} ions in the two positions and explained the polarized absorption spectra in terms of the transitions between the split crystal-field levels. An alternative interpretation was proposed by Runciman et al. (1973), who regarded the Fe2 site as having C_{2v} symmetry.

Burns (1970) attributed the strong peak in the γ spectrum to excitations of the electrons localized at the site Fe2, and both peaks in the α and β spectra to those at the Fe1 site. The present work goes beyond the qualitative analysis based on the idealized models of the Fe ion environment. We numerically solve the Schrödinger equation for a perfect Fe_2SiO_4 crystal without simplifying its crystal structure. We use two complementary approaches: the band-structure concept and the cluster model. The former approach uses as a basis the crystal geometry and atomic constituents and yields the optical spectrum without using any adjustable parameters. However, the intermediate results are given in terms of Bloch

TABLE 1. Coordinates of atomic sites in Fe₂SiO₄

Atom	Number of sites	x	y	z
Fe1	4	0	0	0
Fe2	4	0.9896	0.2803	¼
Si	4	0.4312	0.0976	¼
O1	4	0.7681	0.0922	¼
O2	4	0.2089	0.4536	¼
O3	8	0.2890	0.1656	0.0364

Note: data from Fujino et al. (1981).

FIGURE 1. The total and the partial *l*-projected DOS curves for fayalite. Total DOS = solid line; Si s = dotted-dashed line; *Si* p = long-dashed line; Fel d = dashed line; Fe2 d = dotted line.

functions; this blurs the picture of the splitting of the 3d levels. In contrast, the cluster approach yields energy levels of spatially localized orbitals, which can be directly compared with the prediction of Burns (1970).

In the present work, optical properties of fayalite are calculated on the basis of the one-electron band structure within the local density approximation (LDA) of the density functional theory (DFT) (Hohenberg and Kohn 1964, Kohn and Sham 1965). Several possible errors are associated with this approximation. Within LDA it is impossible to exclude the electron self-interaction, and the energies of the localized electron states may be overestimated (Williams and Barth 1983). In the case of insulators this leads to underestimated values for the calculated band gaps. In Fe-containing minerals an additional difficulty with LDA is that the failure to treat electron correlations properly leads to overestimated Fe-O coupling, thus producing considerable p and f contributions to the Fe 3d wave functions. As a result, and in contrast to the experimental observation, the calculated Fe 3d states do not exhibit an almost pure ionic character. Implications of the observed delocalization of the 3d wave functions are discussed later.

COMPUTATIONAL DETAILS

Band structure calculations

The calculations described here correspond to a temperature of 0 K. At low temperatures the magnetic ordering in fayalite is known to be complex (Fuess 1988). In the present paper, we simplified the problem by choosing a paramagnetic ground state $^1A_{1g}$ configuration instead of the actual $^5T_{2g}$ one. Thus in the present calculations all the t_{2g} states contribute equally to the spectrum as initial states. Therefore, the resultant spectrum has been normalized to the number of transitions corresponding to a $^5T_{2g}$ ground state configuration.

In the present work, we do not take into account the deviations of the one-electron crystal potential from the muffin-tin form. With the muffin-tin radii S_O = 0.79, S_{Si} = 0.87, and S_{Fe} = 1.22 Å, the (touching) spheres comprise ~35% of the unit cell. Our experience with rutile and perovskite structures (Krasovska et al. 1995, 1996) suggests that the muffin-tin approximation is plausible in the case of MO_6 octahedra. The exchange-correlation potential was constructed following Hedin and Lundqvist (1971). To solve the Schrödinger equation we used the
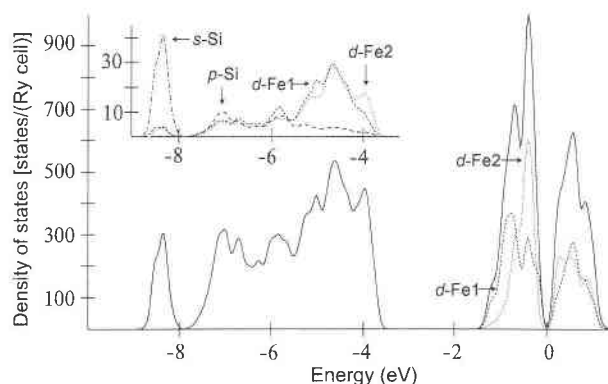
self-consistent, semi-relativistic extended linear-augmented plane-wave method. The formalism of the extended LAPW method was described by Krasovskii and Schattke (1995). We use the Fortran code ELAPW written by one of the authors (E.E.K.). In the present calculation, the ELAPW setup was similar to that used for in the complex oxides (see Krasovska et al. 1995). The electron wave function is a linear combination of 1397 energy independent augmented plane waves (APWs) and 68 localized functions of angular momenta up to l_{max} = 2 for the sphere of Fe, and up to l_{max} = 1 for O and Si. The parameter $|G_{max}| S$ = 5.11, where G_{max} is the longest reciprocal lattice vector used in the APW set and S is the radius of the muffin-tin sphere of O. We calculated the energy band structure of Fe_2SiO_4 over the energy region from O 2s states to 13 eV above the valence band (Fig. 1). All eigenenergies in the interval of interest were converged to within 5 mRy. In constructing the density-of-states (DOS) functions and optical spectra we integrated over the irreducible Brillouin zone (IBZ = ⅛ BZ) using the tetrahedron method of Lehmann and Taut (1972) with a mesh of 115 *k* points (320 tetrahedra) in the IBZ.

The core states were included in the self-consistent procedure and were treated fully relativistically by means of an atomic-like calculation.

Cluster calculation

Xα-SW calculations (Johnson 1966) have been performed to study the splitting of the Fe^{2+} energy levels in FeO_6^{10-} clusters of different symmetry.

The effective potential was obtained self-consistently as a muffin-tin potential with non-overlapping muffin-tin spheres. The exchange-correlation contribution of the form used by Barth and Hedin (1972) was employed. The radii of Fe, O, and Watson's sphere were 1.19, 0.98, and 3.12 Å, respectively. To avoid the unphysical hybridization with electronic states localized outside Watson's sphere, we shifted the potential inside Watson's sphere by −0.5 Ry with respect to the potential outside the sphere.
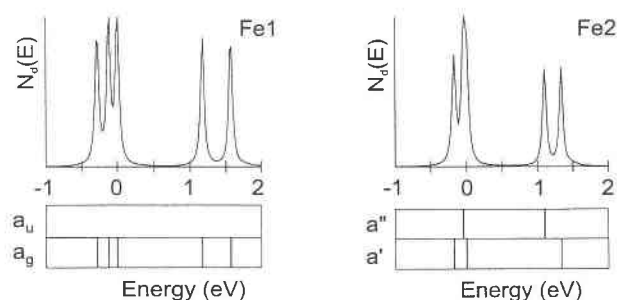
FIGURE 2. The energy-level diagrams for the Fe d states in the FeO$_6^{10-}$ cluster of symmetry C_i (left figure) and C_s (right figure).

TABLE 2. Comparison of the energies (eV) of the Fe^{2+} 3d levels calculated by the Xα-SW method with the model of Burns (1993)

	Fe1 (C_i)		Fe2 (C_s)	
	Present work	Burns (1993)	Present work	Burns (1993)
e_g	1.568 (a$_g$)	1.185	1.334 (a')	0.942
	1.171 (a$_g$)	0.813	1.097 (a'')	0.889
t_{2g}	0.000 (a$_g$)	0.000	0.000 (a')	0.000
	−0.122 (a$_g$)	−0.099	−0.043 (a'')	—
	−0.286 (a$_g$)	−0.186	−0.174 (a')	−0.207

Inside the muffin-tin spheres the cluster wave functions were expanded up to $l_{max} = 2$ for Fe, $l_{max} = 1$ for O, and $l_{max} = 4$ outside Watson's sphere. We use a Xα-SW Fortran code written by one of the authors (A.N.Y.) for the calculations.

The Fe 3d DOS curves in Figure 2 are discrete cluster levels broadened by a Gaussian with a full width at half-maximum (FWHM) of 0.1 eV.

ENERGY BAND STRUCTURE

The total and l-projected partial DOS curves are shown in Figure 1. All the curves are convoluted with a Gaussian with a 0.2 eV FWHM. The energy zero is taken at the valence-band maximum. The present calculation predicts Fe$_2$SiO$_4$ to be an insulator with an indirect forbidden gap of 0.25 eV that separates occupied Fe t_{2g} states (bands 65–88) from unoccupied Fe e_g states (bands 89–104). The bandwidths of the t_{2g} and e_g manifolds are 1.3 eV and 1.25 eV, respectively. The distance between their centers of gravity is ~1 eV. In reciprocal space the top of the valence band is an almost dispersionless band in the direction X-S [X = $2\pi(0.5/a, 0, 0)$; S = $2\pi(0.5/a, 0.5/b, 0)$], and the bottom of the conduction band is also a flat band in the direction Γ-X. We find the valence band maximum at the point S and the conduction band minimum at one-half the distance between Γ and X. The optical measurements by Burns (1970) and Smith and Langer (1982) yield the fundamental absorption edge lower than 0.6 eV; as expected, the local density approximation underestimates the forbidden gap by 50%.

The O 2s states form 16 bands between −21.3 and −19.5 eV. There is a small gap (~0.15 eV) between the fourth and the fifth band, which reflects different surroundings felt by different O atoms.

The O 2p states occupy 48 bands (17–64) between −8.7 and −3.46 eV. They are separated by a gap of 2.2 eV from the Fe t_{2g} manifold; hybridization with the Fe d states is noticeable in the upper part of the O 2p band. The admixture of Si p character is visible in the central part of the O 2p band (from −7.5 to −5.5 eV). The lowermost four bands (17–20) are strongly hybridized with Si 3s states and are separated from the rest of the O 2p states by 0.2 eV (see Fig. 1).

CRYSTAL FIELD SPLITTING OF THE FE 3D LEVELS

The partial 3d DOSs in the spheres of Fe1 and Fe2 (see Fig. 1) have quite different shapes reflecting the different symmetry of the two sites. To study the effect of the O environment in more detail we performed Xα-SW calculations for two FeO$_6^{10-}$ clusters chosen as fragments of the real structure that represent the near environment of Fe1 and Fe2. The experimental atomic coordinates were retained. The energy-level diagrams and corresponding model DOS curves are presented in Figure 2. The energy zero was taken at the top of the t_{2g} manifold. In the Fe1 site, the perfect O_h symmetry was lowered to C_i, which split t_{2g} and e_g states into non-degenerate {a$_g$, a$_g$, a$_g$} and {a$_g$, a$_g$} states, respectively. The symmetry of Fe2 site was lowered to C_s, which splits t_{2g} and e_g states into the singly degenerate {a', a'', a'} and {a'', a'} states, respectively. The energies of the levels are listed in Table 2. The cluster calculation is in good agreement with the predictions of Burns (1993); the Fe1 t_{2g} levels split equidistantly, whereas the upper t_{2g} levels of Fe2 site (a'' and a') are very close; the splitting of e_g levels is larger for the Fe1 site.

The splitting within the manifolds is determined by the symmetry of the environment, whereas the splitting between t_{2g} and e_g manifolds is determined by the volume of the octahedron. The dependence of the t_{2g}-e_g splitting on the Fe-O distance governs the pressure dependence of the main maximum in the optical spectra (see Smith and Langer 1982). To study this in more detail, we performed 22 calculations for clusters of O_h symmetry, varying the Fe-O distance, R, from 2.0 to 2.55 Å. The splitting, ΔE, decreases from 2.0 to 0.7 eV as a power function, $\Delta E = C/R^n$ (Fig. 3). With the parameters $n = 4.35$ and $C = 41$ (ΔE in eV, R in Å) each of the calculated points is reproduced within 0.015 eV. Our result confirms the semi-quantitative derivation of the relationship $\Delta E \approx 1/R^5$ given by McClure (1965). Indeed, in the range of experimentally observed Fe-O distances the deviation from a behavior of $1/R^5$ is negligible. As outlined by Langer (1988) and Burns (1993) this relationship is of fundamental importance in transition-metal geochemistry and in the derivation of the crystal-field–related thermodynamic properties at high pressures.
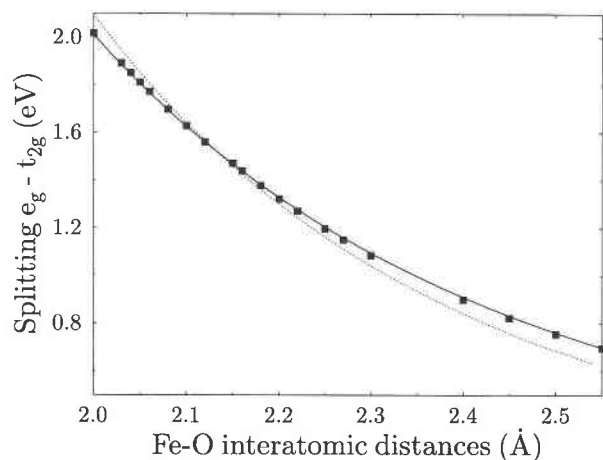
FIGURE 3. Dependence of the splitting between the t_{2g} and e_g multiplets on the Fe-O distance for octahedrally coordinated Fe. The solid line is a fit to the calculated data (squares), with $\Delta E = 41 \times R^{-4.35}$. The dotted line represents a R^{-5} dependence.

FIGURE 4. Imaginary part of the dielectric function of fayalite for three light polarizations in comparison with experimental absorbance spectra of Burns (1970).

OPTICAL SPECTRA

The frequency-dependent dielectric function (DF), $\epsilon_1(\omega) + i\epsilon_2(\omega)$, was calculated within the self-consistent-field one-particle approach of Ehrenreich and Cohen (1959). The imaginary part of the dielectric function is given as:

$$\epsilon_2(\omega) = \frac{8\pi^2 e^2}{m^2\omega^2} \sum_i^{occ} \sum_f^{unocc}$$
$$\int_{BZ} |\mathbf{e}\mathbf{P}_{if}|^2 \, \delta(E_f^k - E_i^k - \hbar h\omega) \frac{d^3\mathbf{k}}{(2\pi)^3} \quad (1)$$

where $\mathbf{e}$ is the polarization vector of the electric field, $\mathbf{k}$ is the point in the IBZ, and E_i and E_f are band energies of the initial and final states. The momentum matrix elements ($\mathbf{P}_{if} = \langle \Psi_{kf} | -i\nabla | \Psi_{ki} \rangle$) were computed as integrals over the unit cell using the formalism described by Krasovskii et al. (1990). There were 150 energy bands considered, of which 88 bands are filled. Because the bands are finite in number the values of $\epsilon_2(\omega)$ are underestimated for $\hbar\omega > 12$ eV, and the spectrum is cut-off at 34 eV.

The absorption coefficient α can be expressed in terms of the dielectric function, DF, (Ehrenreich and Cohen 1959)

$$\alpha(\omega) = \frac{2\omega}{c} \sqrt{\frac{\sqrt{\epsilon_1^2(\omega) + \epsilon_2^2(\omega)} - \epsilon_1(\omega)}{2}} \quad (2)$$

where the real part of the DF, $\epsilon_1(\omega)$, can be calculated by the Kramers-Kronig analysis. The calculated spectrum of the imaginary part of the DF is shown in Figure 4 along with the experimental absorbance spectrum of Burns (1970). The theoretical intensity of the absorption band due to the d-d transitions is incorrect; the infrared band appears to be more intense than the charge-transfer band in the ultraviolet part of the spectrum, whereas the experimental d-d absorption cannot be visible on this scale.
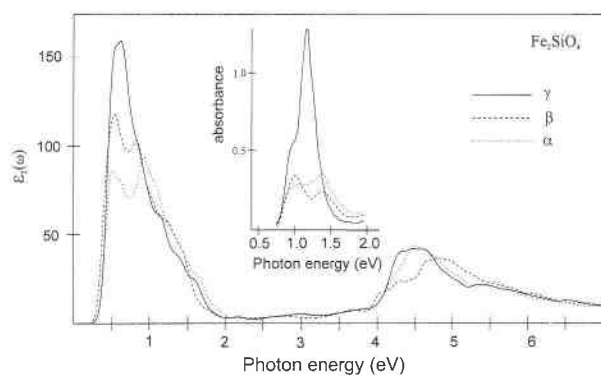
This is not a failure of the computational procedure. The contribution to the left-hand side of the f-sum rule

$$\int_0^\infty \epsilon_2(\omega)\omega \, d\omega = \frac{2\pi^2 e^2}{m} N_{val.\ electr.} \quad (3)$$

from the spectral region $\hbar\omega \leq 34$ eV amounts to 30%, which implies that the basic principles of the one-electron theory are not violated. However, the electron correlations in the Fe 3d shell are strong, and the LDA-based one-electron method appears to be incapable of reproducing the ionic character of the Fe 3d states. As a result, in the present calculation the covalency of the Fe-O bonds is overestimated, thus producing huge transition probabilities.

It follows from the experimental data that the real part of the DF in the infrared region is determined (by means of the Kramer-Kronig relation) by intense absorption bands in the ultraviolet region. Hence, for $\hbar\omega \leq 1.5$ eV, $\epsilon_1(\omega)$ varies slowly, and, taking into account that $\epsilon_2 \ll \epsilon_1$ in this region, we derive from Equation 2 that the absorption coefficient $\alpha(\omega)$ and the absorbance are proportional to $\epsilon_2(\omega)$. Thus in Figure 4 the theoretical ϵ_2 curves are compared with the experimental absorbance spectra. There is a qualitative agreement between theory and experiment in the gross features of the spectra: the γ spectrum is the most intense and has a single well-defined maximum; the α and β spectra both have two maxima, the low-energy maximum being the more intense in the β spectrum and the less intense in the α spectrum. The theoretical spectra are shifted to lower energies by 0.4 eV, which is a typical error of the local density approximation. The low-energy shoulder in the γ spectrum is not resolved in the theoretical curve. On the local basis of the calculated l-projected partial charges of the Bloch states involved in Equation 1, we can elucidate the origin of the main peaks. The present calculation assigns the intense peak in the γ spectrum almost solely to transitions at the Fe2 site. The α and β spectra are mostly due to the transitions at the Fe1 site, however, there is also a considerable contribution from the Fe2 transitions, which we roughly estimate to be 10–30% of the integral intensity.

CONCLUSION

This work is an attempt to apply ab initio quantum-mechanical calculations to interpretation of the experimental absorption spectra of Fe-containing minerals. The band-structure approach yields absorption spectra in satisfactory qualitative agreement with the measurements and supports the interpretation of the spectra proposed by Burns (1970). The cluster calculations, in which true symmetry of the Fe sites was taken into account, yield positions of the 3d levels in accord with those derived by Burns (1970) on the basis of the model considerations.

The present approach dramatically overestimates the intensities of the d-d transitions, which we ascribe to an inadequacy of the one-electron approximation used here. Other approximations used here are presumably less crucial. In particular, it is unlikely that the use of a full potential instead of a muffin-tin potential or the use of a generalized gradient approximation instead of the LDA would lead to results significantly different from those presented here. However, we expect that future development of computational procedures, which would involve excluding the self-interaction and taking into account electron correlations, would improve the results.

REFERENCES

Burns, R.G. (1970) Crystal field spectra and evidence of cation ordering in olivine minerals. American Mineralogist, 55, 1608–1632.
———(1993) Mineralogical applications of crystal field theory. Cambridge University Press, Second Edition, 551 p.
Brown, G.E. Jr (1982) Olivines and silicate spinels. In Mineralogical Society of America Reviews in Mineralogy, 5, 275–392.
Ehrenreich, H. and Cohen, M.A. (1951) The SCF approach to the many-electron problem. Physical Review B, 115, 789–790.
Fujino, K., Sasaki, S., Takeuchi, Y., and Sadanaga, R. (1981) X-ray determination of electron distributions in forsterite, fayalite and thephroite. Acta Crystallographica, B37, 513–518.
Fuess, H., Ballet, O., and Lottermoser, W. (1988) Magnetic phase transitions in olivines M_2SiO_4. In S. Ghose, J.M.D. Coey, E.K.H. Salje, Eds., Structural and magnetic phase transitions, p. 187–207. Springer Verlag, New York.
Hedin, L. and Lundqvist, B.I. (1971) Explicit local exchange-correlation potentials. Journal of Physics, C4, 2064–2083.
Hohenberg, P. and Kohn, W. (1964) Inhomogeneous electron gas. Physical Review, 136, B864–871.
Kohn, W. and Sham, L.J. (1965) Self-consistent equations including exchange and correlation effects. Physical Review, 140, A1133–1137.
Johnson, K.H. (1966) Multiple-scattering model for polyatomic molecules. Journal of Chemical Physics, 45, 3085–3098.
Krasovska, O.V., Krasovskii, E.E., and Antonov, V.N. (1995) Ab initio calculation of optical and photoelectron spectra of RuO_2. Physical Review, B52, 11825–11829.
———(1996) Theoretical study of optical and ultraviolet photoemission spectra of $SrTiO_3$. Solid State Communications, 97, 1019–1023.
Krasovskii, E.E. and Schattke, W. (1995) The extended-LAPW-based $\vec{k}$ * $\vec{p}$ method for complex band structure calculations. Solid State Communications, 93, 775–779.
Krasovskii, E.E., Antonov, V.N., and Nemoshkalenko, V.V. (1990) Microscopic calculation of the interband optical conductivity of ScPd. Physics of Metals, 8, 882–885.
Langer, K. (1988) UV to NIRT spectra of silicate minerals obtained by microscope spectrometry and their use in mineral thermodynamics and kinetics. In E.K.H. Salje, Ed., Physical properties and thermodynamic behaviour of minerals, p. 639–685. Reidel Publishing Company, Dordrecht.
Lehman, G. and Taut, M. (1972) On the numerical calculation of the density of states and related properties. Physica Status Solidi, (b)54, 469–476.
McClure, D.S. (1965) The effects of inner-orbitals on thermodynamic properties. In T.M. Dunn, D.S. McClure and R.G. Pearson, Eds., Crystal field theory, p. 77–95. Harper and Row, New York.
Runciman, W.A., Sengupta, D., and Gourley, J.T. (1973) The polarized spectra of iron in silicates. II. Olivine. American Mineralogist, 58, 451–456.
Schwab, R.G. and Kustner, D. (1977) Prazisionsgitterkonstantenbestimmung zur Festlegung rontgenographischer Bestimmungskurven für synthetische Olivine der Mischkristallreihe Forsterit-Fayalit. Neues Jahrbuch fur Mineralogie, Monatshefte, 5, 205–215.
Smith, H.G. and Langer, K. (1982) Single crystal spectra of olivines in the range 40,000–5,000 cm⁻¹ at pressures up to 200 kbar. American Mineralogist, 67, 343–348.
Von Barth, U. and Hedin, L.A. (1972) A local exchange-correlation potential for the spin polarized case. Journal of Physics, C5, 1629–1642.
Williams, A. and Barth, U. (1983) Application of the Density Functional Theory to Atoms, Molecules, and Solids. In S. Lundqvist and N.H. March, Eds., Theory of the inhomogenius electron gas, p. 189–254. Plenum Press. New York and London.